SOLAR UV TEMPORAL VARIATIONS DURING SOLAR CYCLE 22 & THE TWENTIETH CENTURY

Richard F. Donnelly

Space Environment Lab., NOAA ERL
Boulder, Colorado 80303, U. S. A.

ABSTRACT

Solar ultraviolet measurements of the Mg II core-to-wing ratio from the NOAA9 satellite show a fast rise for solar cycle 22 from the minimum in September 1986. The high values in late 1989 are comparable to the maximum values for cycle 21. Estimates of earlier solar UV variations are made back to 1947 using a combination of the 10 cm solar radio flux (F10) and the sunspot blocking function. The latter is interpreted to partially remove the gyroresonance component from F10, which is not present in the UV flux.

INTRODUCTION

Solar ultraviolet (UV) variations are important to research of the climatic impact of solar variability because the UV flux does the following: (1) influences the solar radiation input to the troposphere; (2) photodissociates the major atmospheric constituents in the stratosphere, which subsequently induce changes in minor constituents that affect atmospheric chemistry and radiation absorption and emission; and (3) heats the stratosphere, which may influence tropospheric as well as stratospheric dynamical processes. In case 1, the solar UV flux variations contribute between one fifth to one third of the solar cycle variation of the total solar irradiance (Lean, 1989; London et al., 1989). This reduces the amplitude of the solar cycle variation of solar radiation reaching the ground compared to the total solar irradiance variations observed from satellites. Also, solar UV intensifications increase the atmospheric columnar ozone content, which enhances atmospheric absorption and further decreases the solar cycle variation of solar radiation reaching the ground.

Heath and Schlesinger (1986) showed that the core-to-wing ratio of the Mg II h & k absorption lines near 280 nm provides a measure of solar UV variability that was insensitive to instrument drift for the Solar Backscatter Ultraviolet (SBUV) observations from the NIMBUS7 satellite. This paper discusses similar Mg II core-to-wing ratios for the rise of solar cycle 22, based on measurements from the SBUV2 monitor on the NOAA9 satellite.

The Ottawa 10.7 cm solar radio flux measurements (F10) have long been used to estimate the temporal variations of solar UV fluxes. Recent studies have shown that the short-term (days, weeks) UV variations differ markedly from those of F10. This paper shows that the long-term variations of F10 and R(MgIIc/w,t) are closely related with a divergence from linearity during the end of the cycle decay into solar minimum. Separating F10 into long-term and short-term variations improves the estimate of UV variations. Including the sunspot blocking function of Hoyt and Eddy (1982) further improves the estimates of short-term UV variations. Their sunspot blocking function sums over the visible solar disk the sunspot umbral and penumbral areas weighted by a contrast function that varies with the angle between the solar radial through the center of the spot and our line of observation. Preliminary estimates for the long-term variations of R(MgIIc/w,t) for solar cycles 18 - 21 are presented.

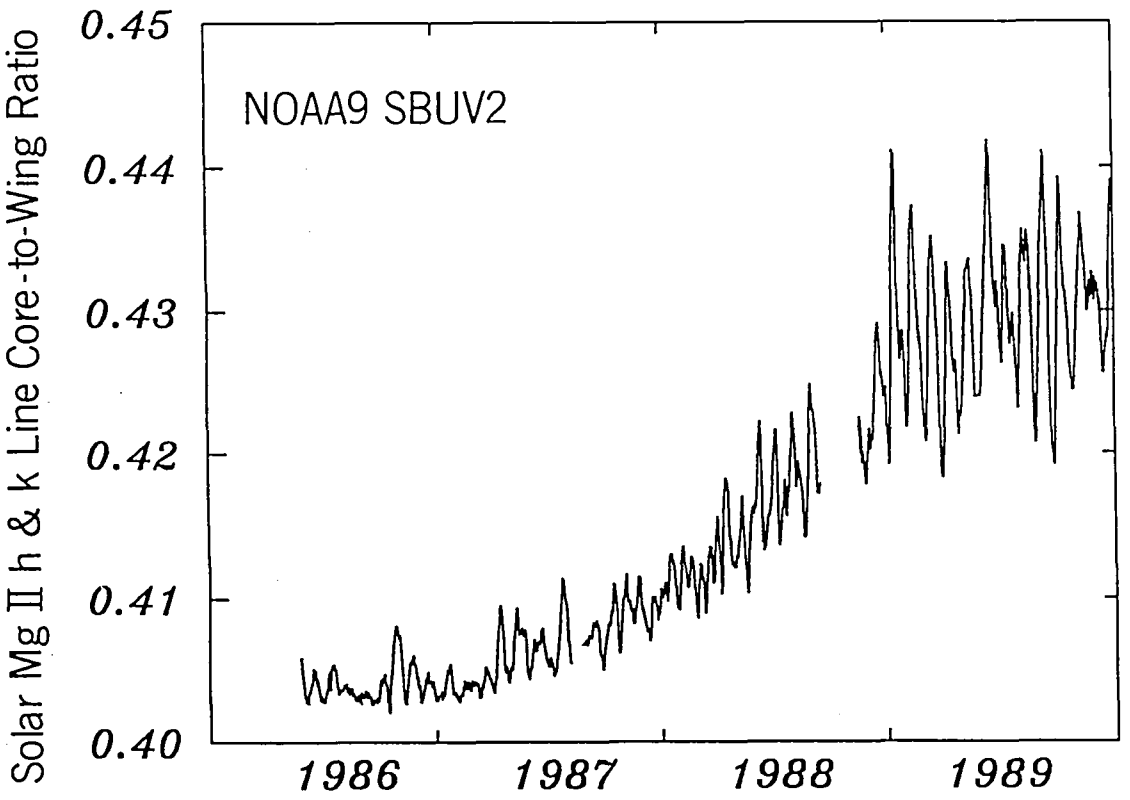

Fig. 1. Daily core-to-wing ratio for the unresolved solar Mg II h & k absorption lines from solar cycle minimum in September 1986 through the rise of solar cycle 22.

THE RISE OF SOLAR CYCLE 22

The Mg II core-to-wing ratio derived from the discrete wavelength measurements of the NOAA9 SBUV2 monitor are shown in Fig. 1 from the solar minimum in 1986 through the rise of solar cycle 22. The ratio shown has been modified with respect to that used by Heath and Schlesinger (1986) for NIMBUS7 in order to limit the NOAA9 measurements to the second of three gain ranges and thereby reduce the day-to-day jitter and long-term drift in the ratio (Donnelly et al., 1990). These NOAA9 results are related to the NIMBUS7 ratios by a simple linear relation that shows the 1989 maximum daily and 81-day average values are approximately equal to the corresponding maximum values from NIMBUS7 for solar cycle 21. Note the very strong solar rotational variations with 27 to 28 days periodicity in 1989 after the main rise of the cycle. These short-term variations have roughly half the amplitude of the long-term rise from the 1986 minimum to the average 1989 level, but are not as large as the solar rotational variations observed by the NIMBUS7 satellite in July and August 1982. An episode of two peaks per solar rotation with weak amplitude occurred in early 1988. The rotational peak in October 1986 resulted from the first episode of strong new-cycle activity for solar cycle 22.

SOLAR CYCLE 21

Fig. 2 shows monthly values of 13-month smoothed (half weight for first and last months) Mg II core-to-wing ratios from the NIMBUS7 satellite. Note how similar are the curves for the chromospheric Mg II ratio R(MgIIc/w,t) and the 10.7 cm solar radio flux (F10) and how those two curves differ greatly from the photospheric sunspot number, coronal green line (G), and soft X-ray flux (X). This similarity between the long-term variations of F10 and R(MgIIc/w,t), which was first noted by Heath and

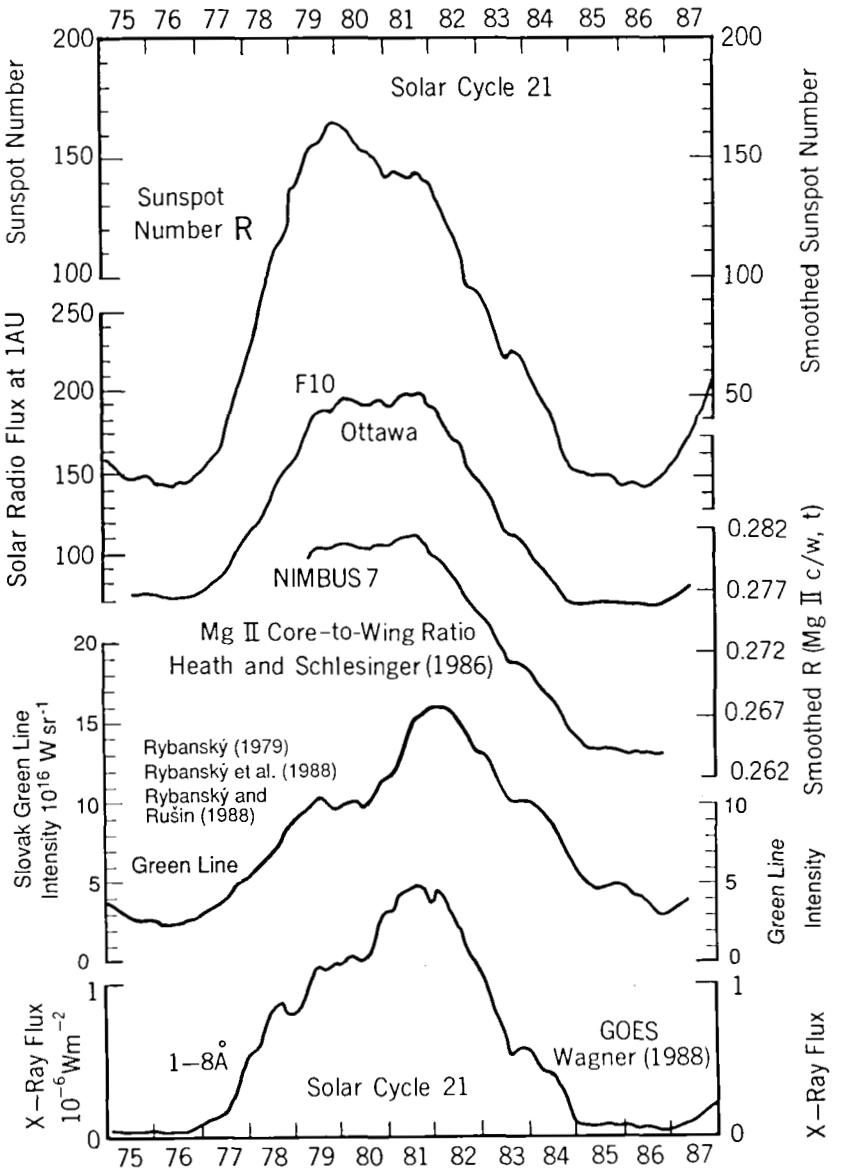

Fig. 2. Smoothed solar cyle 21 variations for the photospheric sunspot number, F10 solar radio flux, chromospheric Mg II core-to-wing ratio, coronal green line effective intensity, and the very hot and active coronal 1 - 8 A flux. The 10.7 cm solar radio flux units (sfu) are 10^{-22} W m^{-2} Hz^{-1}.

Schlesinger (1986), is in stark contrast to the marked differences in their short-term (days, weeks) variations (Donnelly et al., 1983; Donnelly, 1987). However, these long-term variations are not identical. R(MgIIc/w,t) peaks higher in late 1981 relative to the late 1979 level and decays slower in 1985 and early 1986 than F10. Compared to R(MgIIc/w,t) and F10, the sunspot number sharply peaks early and has a long decay while G & X have a strong late peak. F10, R(MgIIc/w,t) and X decay in three years to a flat minimum while G decays slowly until late 1986. The differences in decay and minima behavior of X and G imply corresponding differences in the emission measure in the 1 - 2 x 10^6 range, represented by G, and that at temperatures above 3 x 10^6 K, represented by X.

Differences in short-term variations of daily F10 and R(MgIIc/w,t) are evident in Fig. 3. The range in amplitude of the short-term solar rotational variations is much

larger for F10 relative to the long-term solar cycle amplitude than for R(MgIIc/w,t). The high short-term peaks for F10 tend to be on the first rotation of episodes of major groups of active regions, while R(MgIIc/w,t) tends to peak on the second or sometimes third rotation. During 1985 and 1986, F10 shows fewer rotational peaks than R(MgIIc/w,t), which is a consequence of the UV emission of active regions and their remnants having a much greater persistence (Donnelly, 1987).

The 81-day running averages shown in Fig. 4 suppress the short-term variations and illustrate better the intermediate (months) and long-term variations. The short-term solar-rotational variations are still evident in Fig. 4 in two ways. They contribute the small unimportant 27-day ripples in the curves. Because 27-day variations occur in a series where the peak amplitude per solar rotation quickly rises to a maximum in one or two rotations and then decays over several months, the 81-day running average of these short-term variations will also rise and fall over several months. This second effect contributes part of the intermediate-term (several months) variations shown in Fig. 4. Note that the intermediate-term variations in 1980 and 1981 have a period of roughly half a year and those in 1983 and 1984 are less than a year and may be related to the 155 day and 323 day periodicities in solar activity discussed by Lean and Brueckner (1989) and Pap et al. (1990). The half-year variations in 1980 and 1981 appear to be a little larger, rise faster, peak earlier and decay faster in F10 than in R(MgIIc/w,t), which is consistent with the slower episodic evolution found in the solar-rotational variations in R(MgIIc/w,t). The local valley in F10 near the start of 1982 appears to be filled in by the slower decay in R(MgIIc/w,t). In conclusion, the intermediate-term variations of F10 and R(MgIIc/w,t) are fairly similar, with the shorter periods showing some small differences due to the evolution of major groups of active regions (Donnelly, 1987).

How can the temporal variations of F10 be so different from those of R(MgIIc/w,t) for short-term variations and yet so similar for long-term variations? Consider F10 to consist of three parts, namely: (1) chromospheric thermal bremsstrahlung emission, (2) transition-region and coronal bremsstrahlung emission, and (3) gyroresonance absorption and emission, which are related to the strong magnetic fields from sunspots (Kundu et al., 1980). Because of the greater persistence of plages and their remnants than for sunspots or for hot coronal emissions ($T \geq 3 \times 10$ K), long-term averages are dominated by the chromospheric component. The long-term average of the coronal and gyroresonance components in F10 would produce similar temporal results by reflecting the simple build up and decline of the total amount of activity, except the peak would occur earlier. This shift is caused by their more rapid evolution for each active region. It is consistent with the earlier peak, faster decay and larger amplitude of the half-year variations in 1980 - 1981 in F10 than in R(MgIIc/w,t) in Fig. 4. Considering the much higher peak in late 1981 than the flux level in late 1979 for the coronal green line and 1 - 8 A X-rays in Fig. 2, the combination of the chromospheric bremsstrahlung and gyroresonance components of F10 must be much stronger than the coronal bremsstrahlung.

ESTIMATES FOR SOLAR CYCLES 18 - 21

Given the similarity of long-term variations of F10 and R(MgIIc/w,t) and our current knowledge of their short-term differences, we should be able to make good estimates of R(MgIIc/w,t) back to the beginning of the F10 measurements in 1947. These ratios may then be used with the Heath and Schlesinger's (1986) wavelength scaling function to determine the UV flux variations in the 170 - 290 nm range.

Fig. 5 shows the intensity relation between R(MgIIc/w,t) and F10, where the correlation coefficient (r) is 0.95. There are more points further from the main trend on

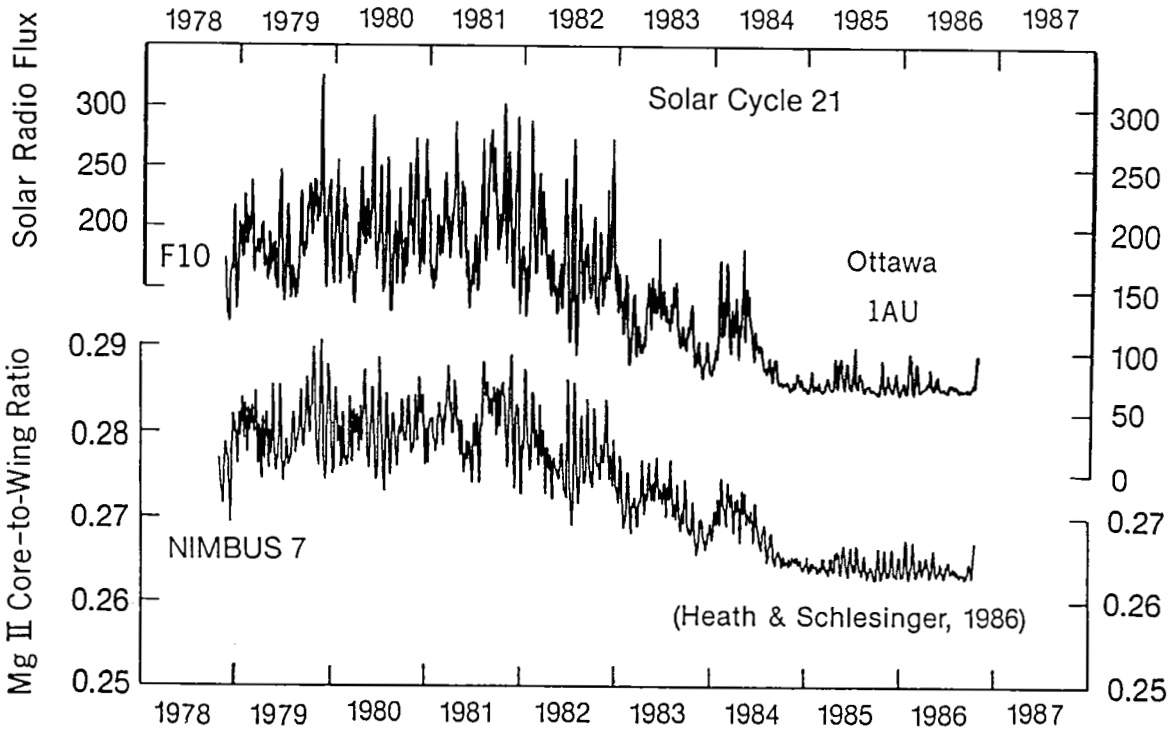

Fig. 3. Daily values of the solar 10.7 cm radio flux and Mg II core-to-wing ratio.

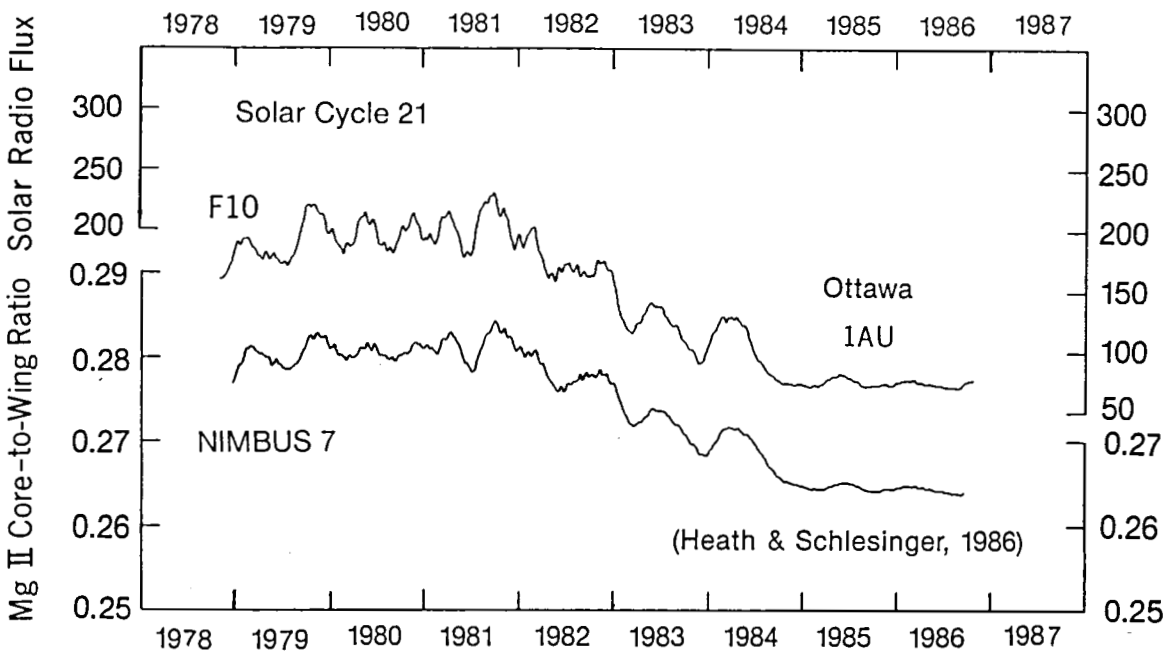

Fig. 4. Daily values of 81-day running averages of F10 and Mg II core-to-wing ratio.

the right side of the diagram, which is caused by the early high solar-rotational peaks in F10 relative to R(MgIIc/w,t) during episodes of major groups of active regions. The most important feature is the break from a linear trend near F10 equal to 94 sfu (solar radio flux units = 10^{-22} W m^{-2} Hz^{-1}). The same type of change in trends near solar minimum was found in Lyman alpha versus F10 by Barth et al. (1990) and is evident in the equivalent width of He I 10830 A (Harvey, 1984) versus F10, except the change is even larger in these two cases. This effect is caused by the slow decay in R(MgIIc/w,t) in 1985 and early 1986 while the minima in F10 per solar rotation are nearly constant. Considering the slow decay in G in Fig. 2 in 1985, we interpret this change in trend to be caused by the gyroresonace component of F10 rather than by the transition-region and coronal component. The data in Fig. 5 were fit with polynomials of order 1 to 7. The best fit was made with two straight lines that join at F10 = 94 sfu. These linear trends were then used with the 81-day average of F10 to make preliminary estimates of the long-term trends of R(MgIIc/w,t) shown in Fig. 6. The maximum estimated values for cycles 18 and 19 are higher than the observed R(MgIIc/w,t) for cycles 21 and 22, at least through 1989.

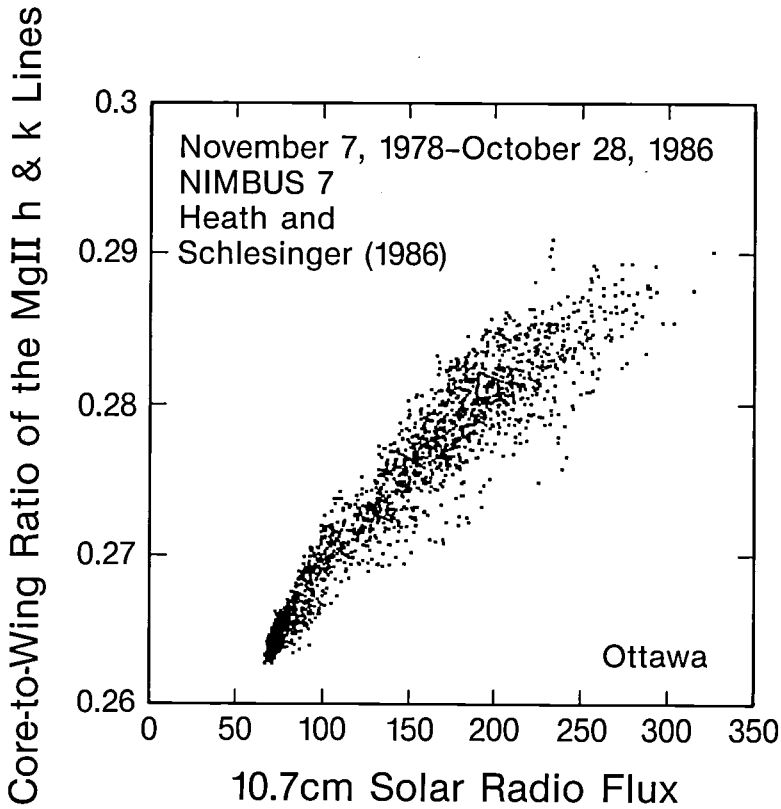

Fig. 5. Scatter diagram of daily values of Mg II core-to-wing ratio versus F10.

In addition to estimating the long-term variations of R(MgIIc/w,t), we have derived techniques for improving estimates of the short-term solar-rotational variations. Simply by separating F10 into long-term and short-term variations improves the estimate because the regression slopes differ for these two time scales. Secondly, including the sunspot blocking function (Hoyt and Eddy, 1982; Hudson et al., 1982) reduces the effect of the large F10 peaks on the first rotation of a major new group of active regions. Oster (1990) has found that the 10 cm enhancement due to an active region is better correlated with that region's sunspot area than with the associated plage area. His result is consistent with the sunspot blocking function improving the fit of F10 with R(MgIIc/w,t). Apparently, the sunspot blocking function provides an approximate correction for the gyroresonance component in F10. This component boosts the radio emission on the first rotation of episodes of major groups of active regions (Donnelly, 1987), when the net sunspot area is large. Another technique for improving the estimate of short-term variations is currently being evaluated. This involves filtering the full-disk Ca-K plage index and sunspot number to identify and estimate episodes of 13-day periodicity, which are strong at UV wavelengths but absent in F10.

Comparing the predicted and observed R(MgIIc/w,t) during the rise of solar cycle 22 has shown that the long-term F10 and R(MgIIc/w,t) trends are related by a small hys-

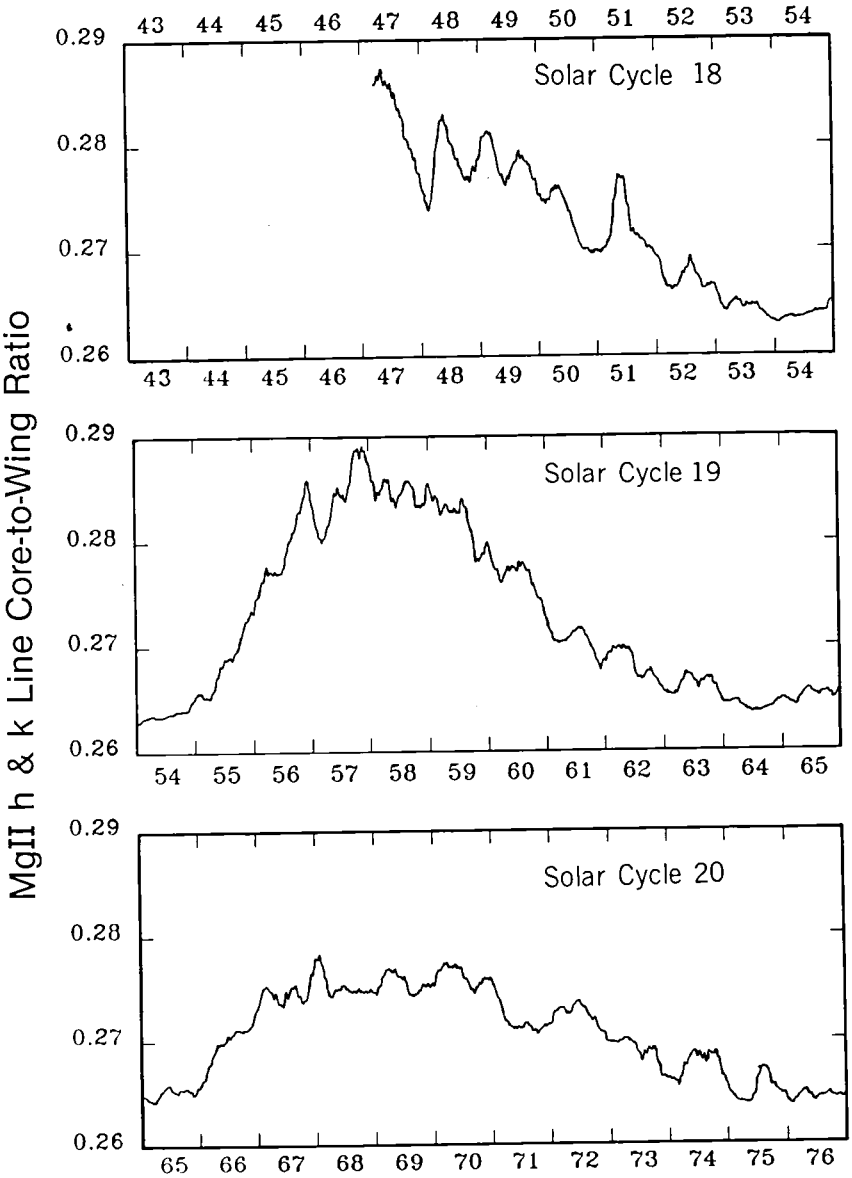

Fig. 6. Preliminary estimates of daily values of 81-day averaged Mg II core-to-wing ratios derived from F10.

teresis effect at low F10 values, which can be accounted for in future estimates. Secondly, using 81-day averages to estimate the long-term variations in R(MgIIc/w,t) from F10 leads to overestimating the intermediate-term variations, especially those with periods near half a year. This can be improved by using annual averages.

CONCLUSIONS

Solar cycle 22 through 1989 at UV wavelengths, as represented by the Mg II core-to-wing ratio, has already reached the peak intensities observed in solar cycle 21, but has not yet reached the peak intensities estimated for solar cycles 18 and 19. Estimates of R(MgIIc/w,t) back to 1947 are currently being developed and improved. Separating F10 into long-term and short-term variations improves the fit to R(MgIIc/w,t). Including the sunspot blocking function improves the estimates of

short-term variations by correcting for the high peaks in F10 relative to R(MgIIc/w,t) during the first solar rotation of an episode of a major group of active regions. These high F10 peaks are interpreted as resulting from the gyroresonance component associated with the strong magnetic fields of sunspots. The sunspot blocking function serves as a measure of the net area of these strong field regions.

REFERENCES

Barth, C. A., W. K. Tobiska, G. J. Rottman, and O. R. White, "Comparison of 10.7 cm Radio Flux with SME Solar Lyman Alpha Flux, Analysis", to be published in Geophys. Res. L., 1990.

Donnelly, R. F., D. F. Heath, J. L. Lean and G. J. Rottman, "Differences in the Temporal Variations of Solar UV Flux, 10.7-cm Solar Radio Flux, Sunspot Number, and Ca-K Plage Data Caused by Solar Rotation and Active Region Evolution", J. Geophys. Res., 88, 9883-9888, 1983.

Donnelly, R. F., J. Barrett, S. D. Bouwer, J. Pap, L. Puga and D. Stevens, Solar UV Flux Measurements from the SBUV2 Monitor on the NOAA9 Satellite, Part I. Mg II h & k Line Core-to-Wing ratios for 1986 - 1987, to be published as a NOAA ERL SEL Tech. Memo., 1990.

Donnelly, R. F., "Temporal Trends of Solar EUV and UV Full-Disk Fluxes", Solar Phys., 109, 37-58, 1987.

Harvey, J., "Helium 10830A Irradiance: 1975-1983", Solar Irradiance Variations on Active Region Time Scales, NASA Conference Publ. 2310, eds. B. J. LaBonte et al., 197-211, 1984.

Heath, D. F., and B. M. Schlesinger, "The Mg 280-nm Doublet as a Monitor of Changes in Solar Ultraviolet Irradiance", J. Geophys. Res., 91, 8672-8682, 1986.

Hoyt, D. V., and J. A. Eddy, An Atlas of Variations in the Solar Constant Caused by Sunspot Blocking and Facular Emissions from 1874 to 1981, NCAR Tech. Note 194+STR, NCAR, Boulder, Colorado, 106 pp, 1982.

Hudson, H. S., S. Silva, M. Woodard, and R. C. Willson, "The effects of sunspots on solar irradiance", Solar Phys., 76, 211-219, 1982.

Kundu, M. R., E. J. Schmahl and M. Gerassimenko, "Microwave, EUV, and X-ray Observations of Active Region Loops: Evidence for Gyroresonance Absorption in the Corona", Astron. Astrophys., 82, 265, 1980.

Lean, J. L., and G. E. Brueckner, "Intermediate-Term Solar Periodicities: 100 to 500 days", Astrophys. J., 337, 568-578, 1989.

Lean, J., "Contribution of Ultraviolet Irradiance Variations to Changes in the Sun's Total Irradiance", Sci., 244, 197-200, 1989.

London, J., J. Pap, and G. J. Rottman, "Observed Solar Near UV Variability: A Contribution to Variations of the Solar Constant", Handbook for MAP, 29, 9-12, 1989.

Oster, L., "Reconstructing the Emission at 10.7 cm from Individual Active Regions in Terms of Optical Data", to be published in J. Geophys. Res., 1990.

Pap, J., W. K. Tobiska, and S. D. Bouwer, "Periodicities of Solar Irradiance and Solar Activity Indices I.", submitted for publication in Solar Phys., 1990.

Rybansky, M., and V. Rusin, private communication, 1988.

Rybansky, M., "Coronal index of solar activity III (Years 1971-1976)", Bull. Astron. Inst. Czechosl., 30, 104-113, 1979.

Rybansky, M., V. Rusin and E. Dzifcakova, "Coronal index of solar activity, V. Years 1977-1986", Bull. Astron. Inst. Czechoslovakia, 39, 106-119, 1988.

Wagner, W.J., "Observations of 1-8A solar x-ray variability during solar cycle 21", Adv. Space Res., 8, (7)67-(7)76, 1988.